0031-3998/08/6302-0158
PEDIATRIC RESEARCH
Vol. 63, No. 2, 2008
Printed in U.S.A.

Probabilistic Brain Tissue Segmentation in Neonatal Magnetic Resonance Imaging

PETRONELLA ANBEEK, KOEN L. VINCKEN, FLORIS GROENENDAAL, ANNEMIEKE KOEMAN, MATTHIAS J. P. VAN OSCH, AND JEROEN VAN DER GROND

Department of Radiology [P.A., K.L.V., A.K.], Department of Neonatology [F.G.], University Medical Center Utrecht, 3584 CX Utrecht, The Netherlands; Department of Radiology [M.J.P.O., J.G.], Leiden University Medical Center, 2300 RC Leiden, The Netherlands

ABSTRACT: A fully automated method has been developed for segmentation of four different structures in the neonatal brain: white matter (WM), central gray matter (CEGM), cortical gray matter (COGM), and cerebrospinal fluid (CSF). The segmentation algorithm is based on information from T2-weighted (T2-w) and inversion recovery (IR) scans. The method uses a K nearest neighbor (KNN) classification technique with features derived from spatial information and voxel intensities. Probabilistic segmentations of each tissue type were generated. By applying thresholds on these probability maps, binary segmentations were obtained. These final segmentations were evaluated by comparison with a gold standard. The sensitivity, specificity, and Dice similarity index (SI) were calculated for quantitative validation of the results. High sensitivity and specificity with respect to the gold standard were reached: sensitivity >0.82 and specificity >0.9 for all tissue types. Tissue volumes were calculated from the binary and probabilistic segmentations. The probabilistic segmentation volumes of all tissue types accurately estimated the gold standard volumes. The KNN approach offers valuable ways for neonatal brain segmentation. The probabilistic outcomes provide a useful tool for accurate volume measurements. The described method is based on routine diagnostic magnetic resonance imaging (MRI) and is suitable for large population studies. **(*Pediatr Res* 63: 158–163, 2008)**

Preterm and full-term neonates admitted to a neonatal intensive care unit carry a high risk of delayed neurodevelopment (1,2). Early identification of patients at risk of neurodevelopmental disabilities may lead to intervention programs and improved outcome (3–5). Although neuromotor development can sometimes be predicted from abnormalities on T2-weighted (T2-w) and inversion recovery (IR) brain MRI, it is impossible to predict mental development from these scans when no abnormalities are visible. It has been suggested that quantitative analysis of MRI might be a better predictor of neurodevelopment than qualitative inspection of T2-w and IR scans (6–9). A suitable method for quantitative analysis is the determination of volumes of brain regions. Therefore, a(n) (semi-)automatic segmentation technique would be highly preferable to achieve reliable and reproducible volume calculations. However, segmentation of the neonatal brain is complicated by the low tissue contrast. Recent methods for adult brain segmentation are often performed on the T1-weighted (T1-w) scan (10–12) or on a combination of T1-w, proton density–weighted (PD), and T2-w MRI (13–16). Still, these approaches cannot be used in neonatal brain segmentation due to anatomical differences and different intensity ranges per tissue type. At present, some neonatal segmentation methods have been described (17–23). All these methods use two or more images from the collection of T1-w, PD, and T2-w. Although these techniques have shown to be useful in neonatal brain research, little is known about the accuracy of the segmentation outcomes and their suitability for volume calculation.

The aim of the present study was to develop an automated, reproducible, probabilistic, and quantitatively validated neonatal brain segmentation algorithm. In this respect, we present this technique for segmentation of white matter (WM), central gray matter (CEGM), cortical gray matter (COGM), and cerebro-spinal-fluid (CSF) regions, based on K-Nearest Neighbor (KNN) classification using information from routine diagnostic T2-w and IR images. The method estimates the probability of voxels being of a particular tissue type.

METHODS

Patients. The study was approved by the Medical Ethical Committee of the Wilhelmina's Children Hospital/University Medical Center Utrecht, and informed consent was obtained in all cases. In the present study, we included 13 newborn children (six males/seven females) who were born and admitted to the neonatal intensive care unit of our hospital between September 2003 and January 2004. MRI was performed for clinical reasons. Only children without cerebral abnormalities on MRI and ultrasonography were included. Median (range) gestational age at birth was 37.1 (25.9–42.9) wk, median postnatal age at test was 2.3 (0.4–17.4) wk, and median corrected age at test was 2.0 (−3.6 to 5.1) wk. Patients breathing spontaneously were sedated using a combination of intramuscular pethidine (2 mg/kg), chlorpromazine (0.5 mg/kg), and promethazine (0.5 mg/kg) (24). Movements were reduced by using vacuum pillows (Med-Tec, Orange City, IA). Patients on mechanical ventilation received morphine (0.1 mg/kg i.v.) and vencuronium (0.1 mg/kg i.v.). Ear cuffs were used to minimize sound exposure. Heart rate and transcutaneous oxygen saturation were monitored using pulse oxymetry (Nonin, Minneapolis, MN) and respiratory rate using an abdominal transducer (Philips Gyroscan ACS-NT, Best, The Netherlands).

MRI. MRI studies were performed on a Philips Gyroscan ACS-NT 1.5-Tesla whole body system (Philips Medical Systems, Best, The Netherlands). All patients were scanned with the same cerebral MR protocol,

Received April 17, 2007; accepted September 19, 2007.

Correspondence: Petronella Anbeek, Ph.D., Department of Radiology, Image Sciences Institute, University Medical Center, Heidelberglaan 100, rm QS.459, 3584 CX Utrecht, The Netherlands; e-mail: P.Anbeek@umcutrecht.nl

Financial support for this study was provided by Philips Medical Systems, Best, The Netherlands.

Abbreviations: CEGM, central gray matter; **COGM,** cortical gray matter; **CSF,** cerebrospinal fluid; **FN,** false negative; **FP,** false positive; **IR,** inversion recovery; **KNN,** K nearest neighbor; **PD,** proton density weighted; **SI,** Dice similarity index; **T1-w,** T1-weighted; **TN,** true negative; **TP,** true positive; **T2-w,** T2-weighted; **WM,** white matter

including a turbo spin echo (TSE) T2-w (repetition time/echo time 7862/150 ms, TSE factor 3), and an IR scan (repetition-time/inversion-time/echo-time 5086/600/30 ms, TSE factor 24). Both scans were performed with 180 × 180-mm field of view, 256 × 256 scan matrix, 50 slices, 2-mm slice thickness, and no slice gap.

Image preprocessing. The segmentation protocol required two preprocessing steps to prepare the data for KNN classification. To correct for differences owing to patient movement, the T2-w and IR image of a patient were coregistered by rigid registration (translation and rotation) (25). To restrict our analyses to brain tissue only, we created a mask denoting the region of interest for the segmentation. This mask was composed by two-means clustering on the voxel intensities of the T2-w image. Two clusters were automatically generated and represented in a binary image, showing two major segments, brain and background, and some smaller segments. Smaller segments inside the brain were added to the brain, and segments outside the brain were added to the background. This resulted in a binary image, called the brain mask.

Manual segmentation and gold standard. Two investigators (P.A. and A.K.) manually segmented the full region inside the brain mask of all patients into four tissue types: WM, COGM, CEGM, and CSF. For each tissue type separately, a threshold was applied on the most relevant scan for that particular tissue type. The binary result was adjusted manually, using the information from the other scans. Next, the four manual segmentations were merged with a priority rule for overlapping voxels: COGM, CEGM, WM, CSF. All voxels within the brain mask were assigned to one of the four tissue classes or to a background class. WM was concerned as one structure, without distinction between myelinated and unmyelinated WM. The cerebellum was not included in the manual segmentation. The manual segmentations were reviewed by two independent experts (F.G. and J.G.), corrected and reevaluated in a consensus meeting, and considered as the gold standard.

KNN classification. The aim of the proposed automatic segmentation method was to determine for each voxel and for each of the four tissue types the probability that the voxel belongs to this specific tissue type. A statistical classification method, called KNN classification, was used for this task. KNN classification is based on the assignment of samples (image voxels) to a class (tissue type) by a search for samples in a learning set with approximately the same features (26). A multidimensional feature space is defined, with each dimension representing a voxel feature. A set of learning samples, *i.e.* the preclassified voxels, is inserted according to their feature values. Next, a new voxel is classified by inspection of the K closest learning voxels in the feature space.

In this study, the learning set for the KNN classification consisted of the manual segmentations, where all voxels inside the brain mask were given a label for one of the four classes: WM, 1; CSF, 2; CEGM, 3; COGM, 4; or background, 0. Owing to the large number of samples, only 20% of the image voxels were randomly selected for inclusion in the learning set, reducing computation time and computer memory usage. Classification of the 13 patients was performed by the so-called leave one out method: each patient was classified based on the learning set composed from the manual segmentations of the other 12 patients.

Two types of features were used: voxel intensity and spatial information features. The first group was defined by the signal intensities of a voxel in the T2-w and IR image. The second feature group incorporated the spatial location of a voxel in the brain. Three spatial features were used, with the values of the x, y, and z coordinate of a voxel in the image. The signal intensities together with the x, y, and z coordinates resulted in a five-dimensional feature space.

Because different features have different ranges, a rescaling of the feature space was performed by variance scaling: subtraction of the feature values by their mean and division by the SD. This resulted in a mean of 0 and variance of 1 for every feature, providing a Mahalanobis distance measure in the feature space (26).

The choice of K in KNN classification depends in general on the number of features and the number of samples. With a small K value, individual samples have more influence on the results. A larger K smoothens the outcome of the classification (26,27). Cover (28) has shown that, for an infinite set of samples, the error rate is R*(1 + 1/k), with R* denoting the Bayes risk (minimum expected risk). This supports the choice for a large K because in this study a relatively large number of samples are invoked. It was observed experimentally that for the current purpose, a K value exceeding 50 had a marginal influence on the accuracy of the classification. Therefore, we concluded that 50 was an acceptable choice for K.

Instead of assigning a voxel to one tissue class, we determined for each tissue type the probability that the voxel belonged to this particular tissue type. This probability was defined as the fraction of voxels of this tissue class among the K neighbors. This resulted in four probabilistic segmentations, one for each tissue type, called probability maps.

Evaluation. From the probability maps, binary segmentations were derived in two different ways. First, by applying thresholds on the probability maps, and, second, by the majority segmentation, each voxel was assigned to the tissue class with the highest probability. Both binary segmentations were compared with the gold standards, where the numbers of true positive (TP), true negative (TN), false positive (FP), and false negative (FN) voxels were determined. For binary segmentations different thresholds, ranging from 0 to 1, and for the majority segmentation, the Dice similarity index (SI) (29) was calculated. This index is a measure for the correctly classified tissue area, where both the FPs and the FNs are taken into account, and is defined by

$$\mathrm{SI} = \frac{2 \times \mathrm{TP}}{2 \times \mathrm{TP} + \mathrm{FP} + \mathrm{FN}}$$

For the binary segmentations with threshold, the maximum SI over all thresholds was determined for each tissue type, and the corresponding threshold was called the optimal threshold. In addition, the sensitivity, TP/(FN + FP), and specificity, TN/(TN + FP), were calculated for the binary segmentation derived with the optimal threshold and for the majority segmentation.

Next, the volumes of the four segmented tissue types and the total brain volume were calculated. All volumes were calculated in three ways: 1) from binary segmentations with the optimal threshold; 2) from the majority segmentation—in both binary segmentations, the volume was calculated by multiplying the number of tissue voxels by the voxel volume; 3) directly from the probabilistic segmentation by multiplying the sum of the probabilities in the probability map by the voxel volume. The total brain volumes were derived by summation of the four tissue volumes. Furthermore, the gold standard volumes of all tissue types and the total brain were calculated from the manual segmentations. For all tissue types, the averages of the three segmentation volumes over all patients were compared with the average gold standard volumes. The differences between the segmentation volumes and the gold standard volumes were compared using the paired-samples t test. A p value <0.05 was considered as statistically significant.

RESULTS

KNN classification was performed for each patient, resulting in four probabilistic segmentations (WM, CSF, CEGM, and COGM) per patient. Figure 1 represents the binary and probabilistic segmentations at the level of the CEGM and at the level of the lateral ventricles. Both examples consist of a T2-w and IR image and two types of segmentations of each tissue type.

The SI has been calculated for thresholds running from 0 to 1 for all tissue types and the optimal thresholds have been determined. Table 1 presents the optimal threshold per tissue type, with the sensitivity, specificity, and SI for the binary segmentation with the optimal threshold and for the majority segmentation. This table shows that the SIs were almost similar in both binary segmentations. The SIs of CSF, WM, and CEGM were between 0.90 and 0.83, whereas the SI of COGM was a little lower (0.74).

The average gold standard volumes, binary segmentation volumes, and probabilistic segmentation volumes of the four tissue types and the total brain were calculated (Table 2). The significance of the binary and probabilistic segmentation volumes with respect to the gold standard was determined by the paired-samples t test. Significant differences ($p < 0.05$) have been indicated. This shows that for WM, COGM, and total brain, the binary segmentation volume with the optimal threshold is significantly overestimated compared with the gold standard volume. For all tissues, except COGM, the majority segmentation volume is significantly overestimated. The volumes derived from the probabilistic segmentations do not show significant differences from the gold standard volumes.

Table 3 represents the probabilistic tissue volumes of all patients separately. The volumes of CEGM, COGM, GM, and total brain are significantly correlated with the corrected age at

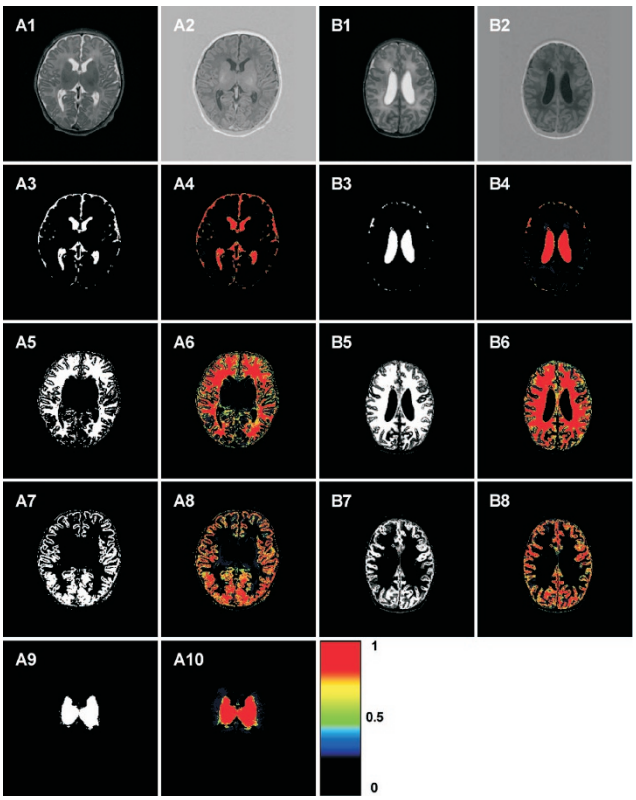

Figure 1. Segmentations of a slice including CEGM (*A*) and one including lateral ventricles (*B*). T2-w image (*1*); IR image (*2*); segmentations of CSF (*3*, *4*); WM (*5*, *6*), COGM (*7*, *8*), and CEGM (*9*, *10*), with the binary segmentation generated from the probability map with the optimal threshold (*left*) and the probabilistic segmentation (*right*).

test. The volumes of WM, total gray matter, and CSF are also shown in Figure 2. Analysis by linear regression showed an increase in volume with respect to the corrected age at test for all tissue categories.

DISCUSSION

KNN classification provides a powerful technique for probabilistic segmentation of brain tissue on neonatal MRI. A single method has been applied for segmentation of four different tissue types simultaneously: WM, CEGM, COGM, and CSF, resulting in high sensitivity and specificity for all tissue classes. The use of separate probability maps for each tissue type provides additional information compared with one overall segmentation image and a large flexibility in the classification and evaluation of the results. Furthermore, brain tissue volumes can be determined accurately from the probabilistic segmentations.

Table 2. *Comparison of average volumes (mL) in classification of four tissue types*

Tissue type	Gold standard	Optimal threshold segmentation	Majority rule segmentation	Probabilistic segmentation
CSF	51.4	54.5	52.6*	51.5
WM	146.4	159.1*	164.9*	151.5
CEGM	20.0	20.5	21.3*	20.7
COGM	101.2	124.1*	118.4	102.3
Total brain	319.0	358.2*	357.1*	326.0

For the binary segmentation volume and probabilistic segmentation volume, the significance level with respect to the gold standard volume was calculated.

* $p < 0.05$, paired-samples t test.

Existing methods for neonatal brain segmentation focus on the segmentation of gray matter, WM, and CSF (17–21); COGM and CEGM (22); or COGM, CEGM, WM, and CSF (23). However, comparison of these methods with our method is difficult because some methods do not evaluate quantitatively or do not have a gold standard; often only visual inspection of the segmentation results is incorporated (17,18,22). Prastawa *et al.* (21) performed quantitative validation, using the SI, on only one slice of the image. However, nothing is known about the difference in segmentation quality among slices. Mewes *et al.* (23) determined the reproducibility of their method but did not quantify the accuracy of the segmentations. Because our method is deterministic, the reproducibility is 100%, whereas in Mewes *et al.* (23), repeated segmentations gave different results. In our study, quantitative validation of the segmentation results of the whole brain, using a binary gold standard, was performed. We evaluated binary segmentations, derived from the probabilistic segmentations in two ways: by applying an optimal threshold to the probability map and by the majority segmentation. Differences in accuracy measures between both binary segmentations were very small. We observed differences in the accuracy results per tissue type. For the CSF, CEGM, and WM, the agreement between the binary segmentations and the gold standard are very high (SI >0.8). The SI of the COGM is slightly lower (0.74), but still indicates an excellent agreement (30). The lower accuracy of the COGM segmentations may be due to the relatively large surface of the segmented area, causing small changes to have large influence on the similarity measures.

The proposed method has been developed for the segmentation of four tissue types in two particular MRI scans (T2-w and IR). These scans were chosen because they have good separating quality of the segmented tissue types. New developments in MRI can bring up more suitable MRI scans.

Table 1. *Similarity measures in classification of four tissue types*

	Optimal threshold segmentation				Majority rule segmentation		
Tissue type	Optimal threshold	Sensitivity	Specificity	SI	Sensitivity	Specificity	SI
CSF	0.38	0.923	0.985	0.899	0.907	0.987	0.897
WM	0.46	0.865	0.920	0.837	0.889	0.906	0.837
CEGM	0.46	0.881	0.994	0.871	0.894	0.993	0.867
COGM	0.38	0.825	0.902	0.742	0.807	0.910	0.739

Table 3. *Tissue volumes relative to ages*

Corrected age at test (wk)	Gestational age at birth (wk)	CSF (mL)	WM (mL)	CEGM* (mL)	COGM† (mL)	Total gray matter† (mL)	Total brain* (mL)
−3.6	34.6	56.8	93.6	15.9	77.6	93.6	244.0
−2.9	36.1	55.9	151.6	18.0	85.9	103.9	311.3
0.7	29.1	51.4	171.5	21.4	112.7	134.1	357.1
0.9	39.6	40.3	169.4	19.8	86.2	106.1	315.8
1.3	33.0	56.5	149.8	21.7	120.7	142.4	348.7
1.9	41.4	50.7	154.8	23.7	102.5	126.2	331.7
2.0	40.9	42.4	177.9	23.8	108.2	132.0	352.3
2.1	41.0	39.2	111.0	15.1	82.8	97.9	248.1
2.9	38.7	39.0	154.1	18.0	107.1	125.1	318.1
3.3	25.9	61.9	152.7	21.9	104.0	126.0	340.5
3.3	30.0	48.4	122.9	20.3	101.3	121.6	292.8
4.0	37.1	52.7	181.9	26.2	111.8	138.0	372.7
5.1	42.9	73.6	178.2	23.4	129.0	152.4	404.2

For all tissue categories, the significance of volume with respect to corrected age at test was calculated. * $p < 0.05$; † $p < 0.01$ (paired-samples t test).

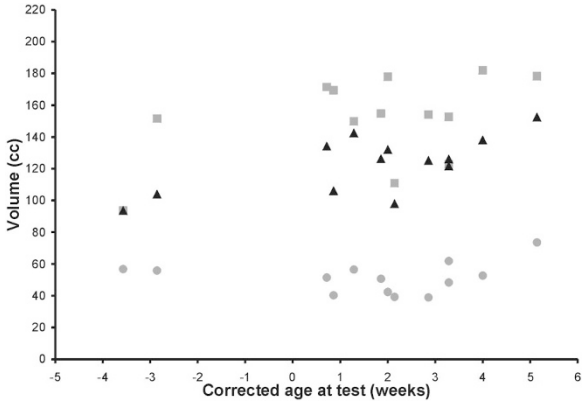

Figure 2. Measured volumes of WM (*squares*), total gray matter (*triangles*), and CSF (*circles*), relative to the corrected age at test. Linear regression showed an increase of volume related to the age for all tissue categories.

Conversely, the T2-w and IR scans may not always be available in clinical practice. When faced with other scans, the same segmentation method can be applied with a new training set, composed of segmentations of the available scans. This training set can be composed manually, in the same way as described in this article. If, besides the new scans, T2-w and IR scans are also available for a small group of patients, a new training set can be composed of the automatic KNN segmentation based on the T2-w and IR scans. It is difficult to predict the accuracy of the proposed KNN segmentation technique with new scans. In general, a more distinctive quality of tissue types, in intensity as well as location, in scans will provide better segmentations.

An issue in neonatal brain segmentation is the discrimination between CEGM and COGM. Both tissue types have a similar intensity range in the IR and the T2-w images for all ages, raising the need for extra information in the segmentation method. The addition of spatial features solved this problem because CEGM and COGM both have a specific location in the brain. The method of Warfield *et al.* (22) also incorporated spatial information in the KNN classification. However, this method implies dependency on a template, constructed from only one patient. This can be problematic in neonatal imaging due to the variety in signal intensity ranges in neonatal brains of different ages. Other existing methods, such as that of Prastawa *et al.* (21), do not differentiate between CEGM and COGM, but differentiate between myelinated and unmyelinated WM. The method of Prastawa *et al.* treats myelination as a fractional property. The MRI intensities reflect the degree of myelination and partial voluming. Furthermore, it deals with significant levels of intensity inhomogeneity and variability due to a combination of radio frequency field (RF) inhomogeneity and biologic properties of the developing tissue and with large overlaps in intensity characteristics of different tissues. This is also possible in the proposed method. The method that differentiates between both myelinated and unmyelinated WM and CEGM and COGM in neonates is that of Hüppi *et al.* (18), which was also used in other studies concerning newborn brain segmentation (8,19,20,23). However, this method is operator dependent and time-consuming. We think that this automatic and user-independent method is promising, with the opportunity of further development for segmenting additional tissue classes, *e.g.* myelinated and unmyelinated WM, the internal capsule, and the cerebellum. They can be included in the training set and be part of the segmentation result. This is important because segmentation of the neonatal brain shows promise to predict long-term outcome in high-risk neonates.

Methods for adult brain segmentation by a multichannel approach (13–16) may be suitable for neonates as well. However, these methods cannot be applied directly to neonatal brains due to significant differences in anatomy and intensity ranges of tissue types. Extra preprocessing steps, like MR inhomogeneity correction and interpatient registration, may be also beneficial to our method. Sample pruning, as proposed by Cocosco *et al.* (16), is less appropriate due to basic differences in the classification of voxels according to the information in the feature space.

It should be noted that the proposed method is insensitive for variations in position in space of the patient's head. The registration step, combined with the use of a brain mask, and the mean and variance scaling of all features correct for differences in location. The difference in head size or shape is also corrected for by this procedure. An interpatient registration step would probably improve resemblance in location, size, and shape. However, preprocessing steps could mean-

while introduce errors by misregistration and interpolation artifacts. Another way to deal with differences is by registration to a brain atlas (21–23). An atlas can be advantageous in the issue of MR inhomogeneity and in discriminating between tissues with similar intensity ranges, as CEGM and COGM. Furthermore, an atlas can be valuable in the study of brain abnormalities by analysis of registration parameters. However, variations in signal intensity between patients of different ages make it difficult to gather a representative patient group fit for the construction of an atlas. Our method is straightforward, easy to implement, and delivers suitable results. Nevertheless, the use of a brain atlas in combination with our method is worth consideration.

A major advantage of this method is the use of spatial information. The tissue probability of a voxel is determined by the signal intensities and by the location of the voxels. The method segments tissues that are heterogeneous in signal intensity like neonatal WM. Although we cannot exclude the influence of intensity-related issues like noise due to the spatial features, the method is less sensitive for it. In previous studies by Aylward and Coggins (31) and Anbeek *et al.* (32), spatial information has been incorporated successfully in the feature space for tissue classification in adult MRI. Other methods for neonatal brain segmentation use a statistical brain atlas to involve location characteristics in the segmentation (21–23). However, the integration of this information by spatial features in the KNN classification is straightforward and easy to apply, reducing the total procedure with another step. Furthermore, the ultimate effect is probably comparable.

Calculation of brain tissue volumes can be performed in different ways using the segmentation outcomes. This study investigated three methods for volume calculation: one derived from the binary segmentation with the optimal threshold, one derived from the majority segmentation, and one derived from the probabilistic segmentation. In both binary segmentations, the volumes of two or more tissue types, and of the whole brain, were significantly different from the gold standard volumes, whereas the probabilistic segmentation volumes did not differ significantly from the gold standard for all tissue types (including the whole brain). This indicates that the probabilistic segmentation volumes provide accurate and robust volume measurements for neonatal brain tissue. The probabilistic volumes of all tissue categories show an increasing trend with respect to the corrected age of the children. For CEGM, COGM, GM, and total brain volume, this increase was significant.

This method has been developed to support other studies concerning the development of children in relation to brain volumes. Therefore, we focused on the segmentation of neonatal brains without obvious abnormalities. Because location is taken into account in the segmentation method, large deformations of brain structures may cause worse results. Other focal abnormalities, as stroke, could be segmented by this method if a specific training set is composed.

The generalizability of the method can be investigated by using some patients for training and the rest of the group for evaluation. The patients used for training should be representative of the whole group to achieve reliable segmentations. The accuracy of the results can be tested by comparison with the manual segmentations.

In conclusion, the KNN approach offers valuable ways to produce segmentations of neonatal brain MRI. The novelty and value of the reported results might appear limited. However, this is a first version of a new reliable method, which is fast, user independent, and 100% reproducible, and can segment different tissues in one run. Our future aim is to improve this segmentation scheme by inclusion of additional tissue classifications, such as myelinated and unmyelinated WM and the cerebellum. The probabilistic outcome provides a useful tool for accurate volume measurements. The method is based on the information from only two routine diagnostic MR scans, and therefore suitable for large and longitudinal population studies. Finally, development of a rapid software tool for neonatal brain segmentation is increasingly relevant for clinical practice. Neonatal brain segmentation has been proven as a promising technique to predict long-term outcome in high-risk neonates (6,33). Based on MRI segmentation findings, neurodevelopmental intervention programs could be initiated.

REFERENCES

1. Hack M, Taylor HG 2000 Perinatal brain injury in preterm infants and later neurobehavioral function. JAMA 284:1973–1974
2. Marlow N, Wolke D, Bracewell MA, Samara M 2005 Neurologic and developmental disability at six years of age after extremely preterm birth. N Engl J Med 352:9–19
3. Resnick MB, Armstrong S, Carter RL 1988 Developmental intervention program for high-risk premature infants: effects on development and parent-infant interactions. J Dev Behav Pediatr 9:73–78
4. McCarton CM, Wallace IF, Bennett FC 1996 Early intervention for low-birth-weight premature infants: what can we achieve? Ann Med 28:221–225
5. 1998 Randomized trial of parental support for families with very preterm children. Avon Premature Infant Project. Arch Dis Child Fetal Neonatal Ed 79:F4–F11
6. Inder TE, Hűppi PS, Warfield S, Kikinis R, Zientara GP, Barnes PD, Jolesz F, Volpe JJ 1999 Periventricular white matter injury in the premature infant is followed by reduced cerebral cortical gray matter volume at term. Ann Neurol 46:755–760
7. Hűppi PS, Inder TE 2001 Magnetic resonance techniques in the evaluation of the perinatal brain: recent advances and future directions. Semin Neonatol 6:195–210
8. Inder TE, Warfield SK, Wang H, Hüppi PS, Volpe JJ 2005 Abnormal cerebral structure is present at term in premature infants. Pediatrics 115:286–294
9. Woodward LJ, Anderson PJ, Austin NC, Howard K, Inder TE 2006 Neonatal MRI to predict neurodevelopmental outcomes in preterm infants. N Engl J Med 355:685–694
10. Chard DT, Parker GJ, Griffin CM, Thompson AJ, Miller DH 2002 The reproducibility and sensitivity of brain tissue volume measurements derived from an SPM-based segmentation method. J Magn Reson Imaging 15:259–267
11. Lemieux L, Hammers A, Mackinnon T, Liu RS 2003 Automatic segmentation of the brain and intracranial cerebrospinal fluid in T1-weighted volume MRI scans of the head, and its application to serial cerebral and intracranial volumetry. Magn Reson Med 49:872–884
12. Shattuck DW, Sandor-Leahy SR, Schaper KA, Rottenberg DA, Leahy RM 2001 Magnetic resonance image tissue classification using a partial volume model. Neuroimage 13:856–876
13. Amato U, Larobina M, Antoniadis A, Alfano B 2003 Segmentation of magnetic resonance brain images through discriminant analysis. J Neurosci Methods 131:65–74
14. Kovacevic N, Lobaugh NJ, Bronskill MJ, Levine B, Feinstein A, Black SE 2002 A robust method for extraction and automatic segmentation of brain images. Neuroimage 17:1087–1100
15. Marroquin JL, Vemuri BC, Botello S, Calderon F, Fernandez-Bouzas A 2002 An accurate and efficient bayesian method for automatic segmentation of brain MRI. IEEE Trans Med Imaging 21:934–945
16. Cocosco CA, Zijdenbos AP, Evans AC 2003 A fully automatic and robust brain MRI tissue classification method. Med Image Anal 7:513–527
17. Toft PB, Leth H, Ring PB, Peitersen B, Lou HC, Henriksen O 1995 Volumetric analysis of the normal infant brain and in intrauterine growth retardation. Early Hum Dev 43:15–29

18. Hűppi PS, Warfield S, Kikinis R, Barnes PD, Zientara GP, Jolesz FA, Tsuji MK, Volpe JJ 1998 Quantitative magnetic resonance imaging of brain development in premature and mature newborns. Ann Neurol 43:224–235
19. Tolsa CB, Zimine S, Warfield SK, Freschi M, Rossignol AS, Lazeyras F, Hanquinet S, Pfizenmaier M, Hűppi PS 2004 Early alteration of structural and functional brain development in premature infants born with intrauterine growth restriction. Pediatr Res 56:132–138
20. Zacharia A, Zimine S, Lovblad KO, Warfield S, Thoeny H, Ozdoba C, Bossi E, Kreis R, Boesch C, Schroth G, Hűppi PS 2006 Early assessment of brain maturation by MR imaging segmentation in neonates and premature infants. AJNR Am J Neuroradiol 27:972–977
21. Prastawa M, Gilmore JH, Lin W, Gerig G 2005 Automatic segmentation of MR images of the developing newborn brain. Med Image Anal 9:457–466
22. Warfield SK, Kaus M, Jolesz FA, Kikinis R 2000 Adaptive, template, moderated, spatially varying statistical classification. Med Image Anal 4:43–55
23. Mewes AU, Hüppi PS, Als H, Rybicki FJ, Inder TE, McAnulty GB, Mulkern RV, Robertson RL, Rivkin MJ, Warfield SK 2006 Regional brain development in serial magnetic resonance imaging of low-risk preterm infants. Pediatrics 118:23–33
24. Groenendaal F, Veenhoven RH, van der Grond J, Jansen GH, Witkamp TD, de Vries LS 1994 Cerebral lactate and N-acetyl-aspartate/choline ratios in asphyxiated full-term neonates demonstrated in vivo using proton magnetic resonance spectroscopy. Pediatr Res 35:148–151
25. Maes F, Collignon A, Vandermeulen D, Marchal G, Suetens P 1997 Multimodality image registration by maximization of mutual information. IEEE Trans Med Imaging 16:187–198
26. Duda RO, Hart PE 2001 Pattern Classification. John Wiley & Sons, New York, pp 174–195
27. Bishop CM. 1995 Neural networks for pattern recognition. Oxford University Press, Oxford, Great Britain, pp 55–59
28. Cover TM 1968 Estimation by the nearest neighbor rule. IEEE Trans Inf Theory 1:50–55
29. Dice LR 1945 Measures of the amount of ecologic association between species. Ecology 26:297–302
30. Bartko JJ 1991 Measurement and reliability: statistical thinking considerations. Schizophr Bull 17:483–489
31. Aylward S, Coggins J 1994 Spatially invariant classification of tissues in MR images. Vis Biomed Comp 2359:353–361
32. Anbeek P, Vincken KL, van Bochove GS, van Osch MJ, van der Grond J 2005 Probabilistic segmentation of brain tissue in MR imaging. Neuroimage 27:795–804
33. Peterson BS, Vohr B, Staib LH, Cannistraci CJ, Dolberg A, Schneider KC, Katz KH, Westerveld M, Sparrow S, Anderson AW, Duncan CC, Makuch RW, Gore JC, Ment LR 2000 Regional brain volume abnormalities and long-term cognitive outcome in preterm infants. JAMA 284:1939–1947